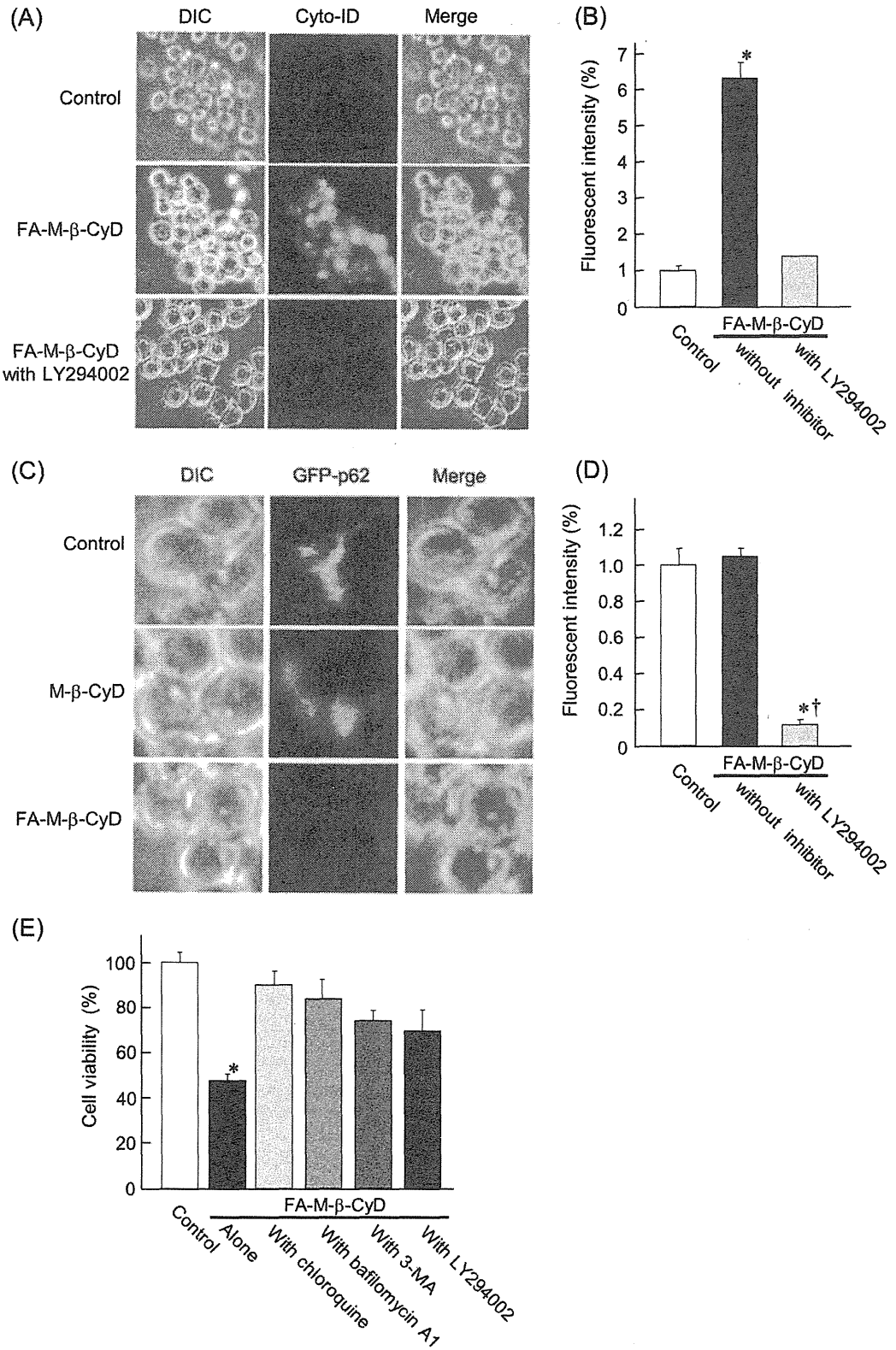

Figure 5 | Induction of autophagy by the treatment of FA-M-β-CyD. (A, B) Effects of FA-M-β-CyD on the autophagosome formation in KB cells. (C, D) Effects of FA-M-β-CyD on the clearance of protein aggregation via autophagy. (E) Effects of chloroquine, bafilomycin A1, 3-MA, and LY294002 on antitumor activity of FA-M-β-CyD for KB cells. Results are represented as mean ± S.E.M. (n = 3–6 per group). $^{*}p < 0.05$ vs. control. $^{\dagger}p < 0.05$ vs. FA-M-β-CyD without inhibitor.

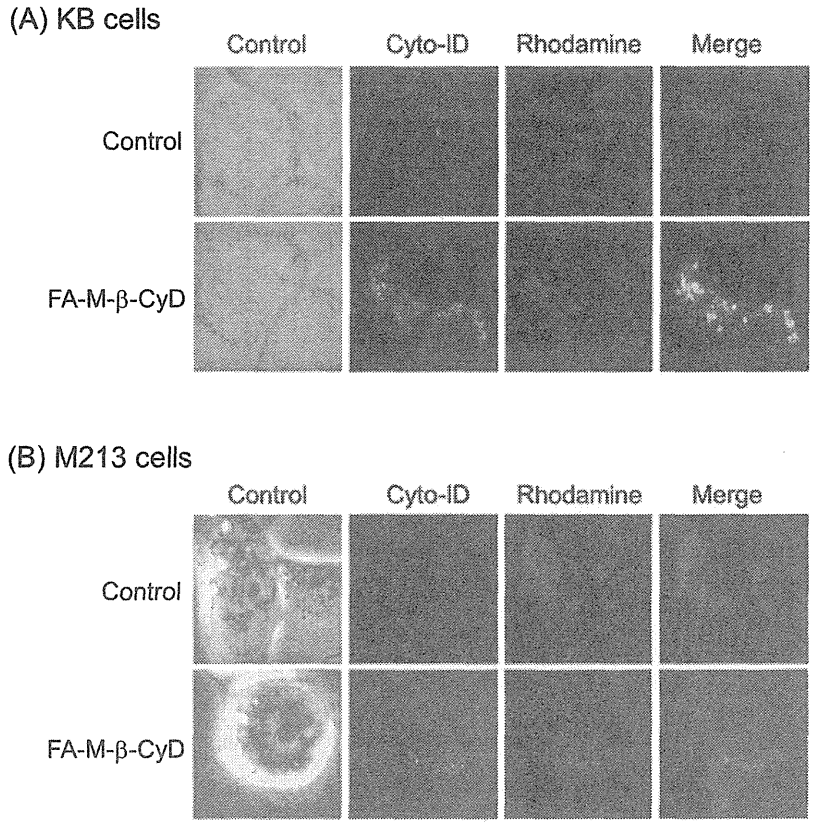

Figure 6 | Colocalization of autophagosomes and mitochondria in KB cells and M213 cells after treatment with FA-M-β-CyD. (A) KB cells and (B) M213 cells were treated with FA-M-β-CyD for 2 h, and then the cells were treated with Cyto-ID™ and rhodamine 123, to stain autophagosomes and mitochondria, respectively.

Recently, an alternative process for controlling cell-death and novel drugs eliciting cancer cell demise have been discovered[31]. Among cell-death machinery, apoptosis plays crucial roles in cell survival and tumor growth. M-β-CyD is often utilized to impair lipid rafts due to the extraction of cholesterol from plasma membranes[15,32]. A number of studies have revealed that M-β-CyD can harm cancer cells through the impairment of lipid rafts. For instance, the decrease in cholesterol level by M-β-CyD provoked apoptosis in human epidermoid carcinoma cells[33]. In addition, we previously reported that DM-β-CyD elicited apoptosis by the impairment of the PI3K-Akt activity, through the depletion of cholesterol from lipid rafts in alveolar macrophages[24]. We also verified that DM-β-CyD provided apoptosis in KB cells through cholesterol depletion (Fig. 4). Additionally, M-β-CyD also elicited apoptosis in KB cells, due to the cholesterol extraction, leading to lowering DNA content in nucleus and transmembrane potential in mitochondria[34]. Interestingly, FA-M-β-CyD significantly released cholesterol from both KB cells (FR-α (+)) and A549 cells (FR-α (−)) to culture medium, compared to that of M-β-CyD and DM-β-CyD in our previous study[18]. However, FA-M-β-CyD showed potent cytotoxic activity without reducing the DNA content in nucleus and transmembrane potential in mitochondria (Fig. 4), suggesting that the cell-death mechanism in FA-M-β-CyD system could be different from apoptosis. Taken together, the modification of FA to M-β-CyD drastically changed the cell-death mechanism, probably due to entry into FR-α-overexpressing cells mediated by CLIC/GEEC endocytosis.

Most importantly, we revealed that involvement of autophagy in cell-death caused by FA-M-β-CyD in FR-α-expressing cells such as KB cells. That is, FA-M-β-CyD enhanced the expression of LC3-II, an autophagosome marker, in autophagic membranes in KB cells (Fig. 5A). Recently, autophagy is thought to be emerging as a key process regulating tumorigenesis and cancer therapy. At the early stage of tumor development, autophagy functions as a tumor suppressor. Meanwhile, at advanced stages of tumor development, autophagy promotes tumor progression. The tumor cells that are located in the central area of the tumor mass undergo autophagy to survive under low-oxygen and low-nutrient conditions. Autophagy protects some cancer cells against anticancer treatment by blocking the apoptotic pathway ('protective autophagy'). In the present study, FA-M-β-CyD was found to induce autophagosome formation in FR-α-positive cells, suggesting the involvement of autophagy in antitumor activity. Taking into the consideration of our previous results that FA-M-β-CyD drastically suppressed the tumor growth in mice inoculated FR-α (+) tumor cells[18], FA-M-β-CyD can be applied as a novel anticancer drug through regulating autophagy for cancer chemotherapy against FR-α-overexpressing tumor. However, it still remains unclear whether FA-M-β-CyD induces the dephosphorylation and inactivation of mTOR, which elicits autophagy, and activates class III PI3K, which involves in the autophagosome formation. Therefore, the further studies on not only the mechanism of autophagy caused by FA-M-β-CyD, but also the contribution of endocytosis pathway to cell-death mechanism are required.

Activation of mitochondrial permeability pore (mPTP) is associated with mitochondrial depolalization, uncoupling of oxidative dephosphorylation, swelling of mitochondria and release of death-promoting factors like cytochrome *c*[35]. Recently, Ziolkowski *et al.* demonstrated that M-β-CyD decreases the function of rat liver mitochondria, and suppresses the calcium chloride-induced swelling[36]. In the present study, FA-M-β-CyD internalized into KB cells may

interact with mitochondrial raft-like microdomains, leading to the suppression of mPTP activity, resulting in the regulation of autophagosome formation. Further elaborate studies regarding the effects of FA-M-β-CyD on mitochondrial function are in progress.

In conclusion, in the present study, we revealed the involvement of autophagy in FR-α-expressing cell-selective antitumor effect of FA-M-β-CyD. These finding will give great information of FA-M-β-CyD as a novel autophagy inducer for cancer chemotherapy.

Methods

Materials. RPMI-1640 (FA-free) was obtained from GIBCO (Tokyo, Japan). Tetramethylrhodamine isothiocyanate (TRITC) and FR-α siRNA (sc-39969) were purchased from Funakoshi (Tokyo, Japan) and Santa Cruz Biotechnology (Delaware, CA), respectively. Lipofectamine™2000 reagent and Premo™ Autophagy Sensors were obtained from Invitrogen (Tokyo, Japan). Cyto-ID® Autophagy Detection Kit was purchased from Enzo Life Sciences (Farmingdale, NY).

Cell culture and *In vitro* antitumor activity. KB cells, a human oral squamous carcinoma cell line, A549 cells, a human lung carcinoma, and M213 cells, a human cholangiocarcinoma cell line, were cultured as reported previously[17]. The antitumor activity *in vitro* was performed by the WST-1 method, as reported previously[18]. Briefly, KB cells, M213 cells and A549 cells (5×10^4/96-well microplate) were treated with 150 μL of culture medium containing 10 mM FA-M-β-CyD for 2 h at 37°C. In the autophagy inhibitory study, KB cells were pretreated with RPMI-1640 culture medium containing 20 μM chloroquine, 1 nM bafilomycin A1, 5 mM 3-methyladenine (3-MA), and 50 μM LY294002 for 24 h. After washing with PBS (pH 7.4), 100 μL of fresh HBSS (pH 7.4) was supplemented. Then, the plates and incubated with WST-1 reagent for 30 min. The absorption wavelength and reference wavelength were 450 nm and 630 nm, respectively.

Cellular association of FA-M-β-CyD. KB cells and M213 cells (1×10^6/35 mm dish) were incubated with 1 mL of culture medium (FA-free) containing 10 μM tetramethylrhodamine isothiocyanate (TRITC)-labeled FA-M-β-CyD (TRITC-FA-M-β-CyD) at 37°C for 1 h. After washing with PBS (pH 7.4), the cells were scraped with 1 mL of PBS (pH 7.4). Data were obtained for 1×10^4 cells on a FACS Calibur flow cytometer using CellQuest software (Becton-Dickinson, Mountain View, CA).

Intracellular distribution of FA-M-β-CyD. KB cells (1×10^6/35 mm glass bottom dish) were treated with 10 μM TRITC-FA-M-β-CyD at 37°C for 1 h. Hoechst 33342 (10 μg/mL) was incubated at 37°C for 10 min. After washing with PBS (pH7.4), RPMI-1640 (FA-free) was added. KEYENCE Biozero BZ-8000, a fluorescence microscope, was used for the detection of TRITC and Hoechest33342.

DNA content and mitochondrial transmembrane potential. The DNA content and transmembrane potential in mitochondria in KB cells were determined as reported previously[34]. Briefly, KB cells (1×10^6/35 mm dish) were treated with RPMI-1640 (FA-free) containing 10 mM DM-β-CyD or FA-M-β-CyD for 2 h. Propidium iodide (PI, 20 μg/mL) and rhodamine 123, the indicators of DNA content and transmembrane potential in mitochondria, respectively, were quantified using a FACS Calibur flow cytometer with CellQuest software.

TUNEL assay. Detection of apoptosis was done by TUNEL assay. In short, KB cells (1×10^6/35 mm glass bottom dish) were incubated with 5 mM DM-β-CyD or FA-M-β-CyD at 37°C for 1 h. The cells were washed with PBS and fixed by incubation in 4% paraformaldehyde in PBS for 1 hr at room temperature. Terminal deoxynucleotidyl transferase (TdT)-mediated dUTP nick and labeling (TUNEL) assays were performed by using the TACS® 2 TdT-DAB in situ Apoptosis Detection Kit (Trevigen Inc., Gaithersburg, MD) according to the manufacturer's instructions.

Cleaved caspase 3 assay. Caspase 3 cleavage assay was performed by western blotting. Briefly, KB cells (1×10^6/35 mm dish) were incubated with RPMI-1640 culture medium (FA-free) containing 10 mM DM-β-CyD or FA-M-β-CyD for 2 h. After washed with PBS, cells were lysed with 4× sample buffer (8% SDS, 40% glycerol, 24% β-mercaptoethanol in Tris-HCl buffer (pH6.8)) and boiled for 5 min. After determining protein concentrations using the bicinchoninic acid reagent from Pierce Chemical (Rockford, IL), samples (20 μg as proteins) were separated with 12% SDS-PAGE and transferred onto Immobilon P membranes (Nihon Millipore, Tokyo, Japan). The membranes were blocked with 5% skim milk in PBS containing 0.1% Tween 20 (PBS-T) and incubated with caspase 3 antibody (Santa Cruz, Delaware, CA) at 4°C for overnight. After washing with PBS-T, the membranes were incubated with secondary antibody of peroxidase-conjugated sheep (Amersham-pharmacia Biotech, Buckinghamshire, UK). Specific bands were detected using an ECL Western blotting analysis kit (Amersham Bioscience, Tokyo, Japan). The bands were detected using the Lumino-image analyzer LAS-1000 plus (Fujifilm, Tokyo, Japan). The band intensity ratio of cleaved caspase 3/pro-caspase 3 was analyzed by Image-J software.

Autophagosome formation. Briefly, KB cells (1×10^6/35 mm dish) were incubated with FA-M-β-CyD (5 mM) for 2 h, in the presences and absence of pretreatment with 1 μM LY294002, an autophagic inhibitor, for 4 h, and then the cells were treated with Cyto-ID® Autophagy Detection Kit. A fluorescence microscope of Biozero BZ-8000 (KEYENCE) was used for cell observation.

Clearance of protein aggregates via autophagy. The clearance of protein aggregates via autophagy was evaluated by the Premo™ Autophagy Sensors. Briefly, the cells (5×10^5/35 mm glass bottom dish) were incubated with RPMI-1640 culture medium (FA-free) for 24 h. After washing with PBS, 25 μL of GFP-p62 was added to the culture medium. After incubation for 16 h, the cells were washed with PBS and incubated with 50 μM chloroquine for 10 h. Then, the cells were incubated with 5 mM FA-M-β-CyD in the presence of 50 μM chloroquine for 2 h. After washing with RPMI-1640 culture medium (FA-free), a fluorescence microscope of Biozero BZ-8000 (KEYENCE) was used for cell observation.

Statistics. All experiments were performed in triplicate in each series of measurements, and each series was repeated more than three times. The experimental results are shown as means ± S.E.M. Significance levels for comparisons between samples were determined with Scheffe's test. The level of statistical significance was set at $P < 0.05$.

1. Chen, H., Ahn, R., Van den Bossche, J., Thompson, D. H. & O'Halloran, T. V. Folate-mediated intracellular drug delivery increases the anticancer efficacy of nanoparticulate formulation of arsenic trioxide. *Mol. Cancer Ther.* **8**, 1955–1963 (2009).
2. Gabizon, A. *et al.* Improved therapeutic activity of folate-targeted liposomal doxorubicin in folate receptor-expressing tumor models. *Cancer Chemother. Pharmacol.* **66**, 43–52 (2010).
3. Lu, Y. & Low, P. S. Folate-mediated delivery of macromolecular anticancer therapeutic agents. *Adv. Drug Deliv. Rev.* **54**, 675–693 (2002).
4. Mi, Y., Liu, Y. & Feng, S. S. Formulation of Docetaxel by folic acid-conjugated d-α-tocopheryl polyethylene glycol succinate 2000 (Vitamin E TPGS(2k)) micelles for targeted and synergistic chemotherapy. *Biomaterials* **32**, 4058–4066 (2011).
5. Nukolova, N. V., Oberoi, H. S., Cohen, S. M., Kabanov, A. V. & Bronich, T. K. Folate-decorated nanogels for targeted therapy of ovarian cancer. *Biomaterials* **32**, 5417–5426 (2011).
6. Antony, A. C. The biological chemistry of folate receptors. *Blood* **79**, 2807–2820 (1992).
7. Low, P. S. & Kularatne, S. A. Folate-targeted therapeutic and imaging agents for cancer. *Curr. Opin. Chem. Biol.* **13**, 256–262 (2009).
8. Limmon, G. V. *et al.* Scavenger receptor class-A is a novel cell surface receptor for double-stranded RNA. *FASEB J.* **22**, 159–167 (2008).
9. Parker, N. *et al.* Folate receptor expression in carcinomas and normal tissues determined by a quantitative radioligand binding assay. *Anal. Biochem.* **338**, 284–293 (2005).
10. Szente, L. & Szejtli, J. Highly soluble cyclodextrin derivatives: chemistry, properties, and trends in development. *Adv. Drug Deliv. Rev.* **36**, 17–28 (1999).
11. Uekama, K. & Otagiri, M. Cyclodextrins in drug carrier systems. *Crit. Rev. Ther. Drug Carrier Syst.* **3**, 1–40 (1987).
12. Motoyama, K. *et al.* Effect of 2,6-di-*O*-methyl-α-cyclodextrin on hemolysis and morphological change in rabbit's red blood cells. *Eur. J. Pharm. Sci.* **29**, 111–119 (2006).
13. Motoyama, K. *et al.* Involvement of lipid rafts of rabbit red blood cells in morphological changes induced by methylated β-cyclodextrins. *Biol. Pharm. Bull.* **32**, 700–705 (2009).
14. Ohtani, Y., Irie, T., Uekama, K., Fukunaga, K. & Pitha, J. Differential effects of α-, β- and γ-cyclodextrins on human erythrocytes. *Eur. J. Biochem.* **186**, 17–22 (1989).
15. Galbiati, F., Razani, B. & Lisanti, M. P. Emerging themes in lipid rafts and caveolae. *Cell* **106**, 403–411 (2001).
16. Grosse, P. Y., Bressolle, F. & Pinguet, F. Antiproliferative effect of methyl-β-cyclodextrin *in vitro* and in human tumour xenografted athymic nude mice. *Br. J. Cancer* **78**, 1165–1169 (1998).
17. Onodera, R., Motoyama, K. & Arima, H. Design and evaluation of folate-appended methyl-β-cyclodextrin as a new antitumor agent. *J. Incl. Phenom. Macrocycl. Chem.* **70**, 321–326 (2011).
18. Onodera, R., Motoyama, K., Okamatsu, A., Higashi, T. & Arima, H. Potential use of folate-appended methyl-β-cyclodextrin as an anticancer agent. *Sci. Rep.* **3(1109)**, 1–9 (2013).
19. Liang, C. *et al.* Autophagic and tumour suppressor activity of a novel Beclin1-binding protein UVRAG. *Nat. Cell Biol.* **8**, 688–699 (2006).
20. Liu, E. Y. & Ryan, K. M. Autophagy and cancer--issues we need to digest. *J. Cell Sci.* **125**, 2349–2358 (2012).
21. Qu, X. *et al.* Promotion of tumorigenesis by heterozygous disruption of the beclin 1 autophagy gene. *J. Clin. Invest.* **112**, 1809–1820 (2003).
22. Takahashi, Y. *et al.* Bif-1 interacts with Beclin 1 through UVRAG and regulates autophagy and tumorigenesis. *Nat. Cell Biol.* **9**, 1142–1151 (2007).
23. White, E. Deconvoluting the context-dependent role for autophagy in cancer. *Nat. Rev. Cancer* **12**, 401–410 (2012).
24. Motoyama, K. *et al.* Involvement of PI3K-Akt-Bad pathway in apoptosis induced by 2,6-di-*O*-methyl-β-cyclodextrin, not 2,6-di-*O*-methyl-α-cyclodextrin, through cholesterol depletion from lipid rafts on plasma membranes in cells. *Eur. J. Pharm. Sci.* **38**, 249–261 (2009).

25. Kondo, Y., Kanzawa, T., Sawaya, R. & Kondo, S. The role of autophagy in cancer development and response to therapy. *Nat. Rev. Cancer.* **5**, 726–734 (2005).
26. Geetha, T. & Wooten, M. W. Structure and functional properties of the ubiquitin binding protein p62. *FEBS Lett.* **512**, 19–24 (2002).
27. Pankiv, S. *et al.* p62/SQSTM1 binds directly to Atg8/LC3 to facilitate degradation of ubiquitinated protein aggregates by autophagy. *J. Biol. Chem.* **282**, 24131–24145 (2007).
28. Kim, I., Rodriguez-Enriquez, S. & Lemasters, J. J. Selective degradation of mitochondria by mitophagy. *Arch. Biochem. Biophys.* **462**, 245–253 (2007).
29. Rodriguez-Hernandez, A. *et al.* Coenzyme Q deficiency triggers mitochondria degradation by mitophagy. *Autophagy* **5**, 19–32 (2009).
30. Doherty, G. J. & McMahon, H. T. Mechanisms of endocytosis. *Annu. Rev. Biochem.* **78**, 857–902 (2009).
31. Long, J. S. & Ryan, K. M. New frontiers in promoting tumour cell death: targeting apoptosis, necroptosis and autophagy. *Oncogene* **31**, 5045–5060 (2012).
32. Simons, K. & Ehehalt, R. Cholesterol, lipid rafts, and disease. *J. Clin. Invest.* **110**, 597–603 (2002).
33. Park, E. K. *et al.* Cholesterol depletion induces anoikis-like apoptosis via FAK down-regulation and caveolae internalization. *J. Pathol.* **218**, 337–349 (2009).
34. Onodera, R. *et al.* Involvement of cholesterol depletion from lipid rafts in apoptosis induced by methyl-β-cyclodextrin. *Int. J. Pharm.* **452**, 116–123 (2013).
35. Bernardi, P., Scorrano, L., Colonna, R., Petronilli, V. & Di Lisa, F. Mitochondria and cell death. Mechanistic aspects and methodological issues. *Eur. J. Biochem.* **264**, 687–701 (1999).
36. Ziolkowski, W. *et al.* Methyl-β-cyclodextrin induces mitochondrial cholesterol depletion and alters the mitochondrial structure and bioenergetics. *FEBS Lett.* **584**, 4606–4610 (2010).

Acknowledgments

This work was funded by a Japan Society for the Promotion of Science (Grant-in-Aid for Young Scientists (B) (25870537)), a Ministry of Health Labour and Welfare (Grant-in-Aid for Third Term Comprehensive Control Research for Cancer program (24100701)), and The Japan Science Society (Sasakawa Scientific Research Grant).

Author contributions

R.O., K.M., N.T., A.O. and A.O. performed the experiments. R.O., K.M., T.H., R.K., S.O. and H.A. analysed the data. R.O., K.M. and H.A. designed the research. K.M., R.O. and H.A. wrote this manuscript. H.A. supervised this work.

Additional information

Supplementary information accompanies this paper at http://www.nature.com/scientificreports

Competing financial interests: The authors declare no competing financial interests.

How to cite this article: Onodera, R. *et al.* Involvement of Autophagy in Antitumor Activity of Folate-appended Methyl-β-cyclodextrin. *Sci. Rep.* 4, 4417; DOI:10.1038/srep04417 (2014).